Atlas based segmentation (integration to the EM algorithm)

Lab 2

Franky E., Gonzalez J.

Prepared for Medical Imaging Registration and Applications, MAIA/MIC MASTERS
November 2023

Contents

1 Introduction

The characterization and differentiation of brain main tissues are fundamental for a wide range of clinical and research applications, necessitating the creation of detailed brain maps or atlases. In this project, we aim to construct a probabilistic brain atlas, which is a sophisticated tool that transcends traditional deterministic atlases by encapsulating the likelihood of tissue types at each voxel within the brain. Leveraging a dataset of labeled brain volumes, our endeavor involves the development and implementation of an algorithm capable of integrating these inputs to generate a probabilistic atlas. This atlas comprises two components: an intensity volume that provides a standard template for the spatial registration of new, unlabeled brain volumes and a probabilistic label volume that represents the statistical occurrence of WM, GM, and CSF across the voxel grid.

1.1 Problem definition

To standardize and align the diverse set of brain images, we employ 'elastix', a robust open-source toolbox, to perform both rigid and nonrigid image registration, ensuring that the spatial correspondences across individual brains are maintained. The resultant atlas is not merely a static representation but a dynamic model that can be utilized to classify tissue types in new brain scans, thereby enhancing the accuracy and efficiency of neuroimaging studies. This report details the methodologies adopted in the creation of the probabilistic brain atlas and discusses the potential implications and applications of this pivotal tool in the field of neuroimaging.

2 Design and implementation of the proposed solution

2.1 Fixed Image Candidate Selection

The establishment of a reliable reference image is a pivotal step in the construction of a probabilistic atlas. This reference, or fixed image, serves as the benchmark for registering all other brain volumes, known as moving images. The most straightforward method of choosing this fixed image is to select one at random from the dataset. However, a more discerning approach is to evaluate all potential candidates against a set of criteria to ensure a more robust atlas construction.

In pursuit of a more refined selection process, we employed the provided code in the `utilities.py` file to scrutinize the dimensions, specifically the Y-axis size, of each brain volume in our dataset. This examination revealed variabilities among the images as seen in table 1, pinpointing the Y-axis to differentiate. Initially, our selection strategy converged on an image corresponding to median Y-axis size seen in the histogram (Fig. **??**), hypothesizing that it would serve as an appropriate central tendency representative for our atlas.

Table 1: Y-axis Sizes of Brain Volume Images

File Name	**Y-axis Size**
1000_1C.nii.gz	287
1001_1C.nii.gz	261
1002_1C.nii.gz	277
1006_1C.nii.gz	312
1007_1C.nii.gz	320
1008_1C.nii.gz	274
1009_1C.nii.gz	295
1010_1C.nii.gz	264
1011_1C.nii.gz	287
1012_1C.nii.gz	295
1013_1C.nii.gz	302
1014_1C.nii.gz	307
1015_1C.nii.gz	319
1017_1C.nii.gz	269
1036_1C.nii.gz	334

Table 2: Statistical Summary of Y-axis Sizes

Measure	**Value**
Mean Y-axis Size	293.53
Median Y-axis Size	295.00

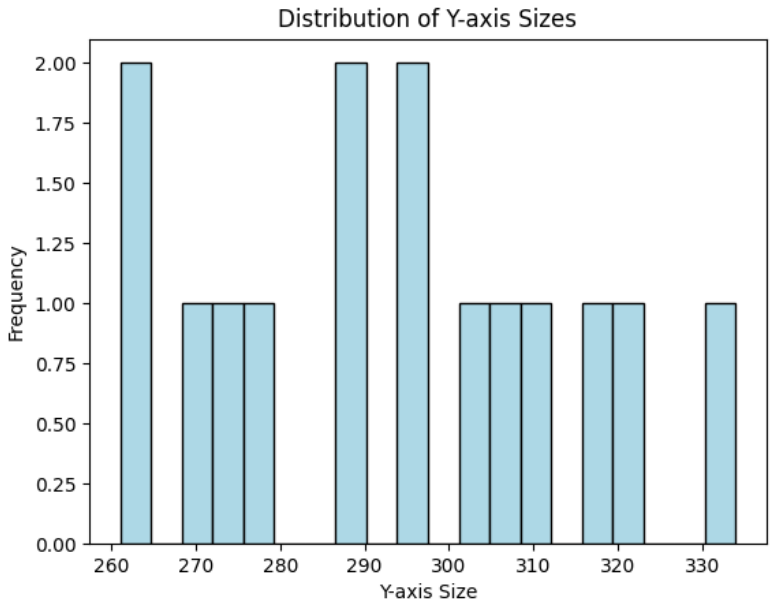

Figure 1: Histogram of Y-axis values of images

To substantiate this preliminary choice, we progressed to a more quantifiable measure: the Dice coefficient score as we have been using it in previous labs in registration and segmentation. The Dice coefficient score—a statistical validation metric for image segmentation —facilitates the assessment of spatial overlap accuracy between two samples. By computing the mean Dice score for each image, juxtaposed against all others in the cohort while deliberately excluding self-comparison, we aimed to identify the image that inherently aligns best with the rest of the dataset.

This computational analysis culminated in the selection of image 1012, which exhibited the highest mean Dice score, indicative of its superior congruence with the collective image properties, despite the absence of any preceding registration efforts. Intriguingly, this image also aligned with the median Y-axis value, thereby confirming our initial intuition with

empirical evidence. Consequently, image 1012 was designated as the optimal fixed image candidate for the subsequent stages of probabilistic atlas development.

2.2 Elastix and Transformix

`Elastix` and `transformix` are two powerful tools widely used in the field of medical image processing, particularly for the tasks of image registration.

`Elastix` is a software package that facilitates the alignment of images, a process known as image registration. It supports various modes of transformation, from rigid to nonrigid, allowing for the precise overlay of images. The transformations that elastix computes can correct for differences in image position, orientation, and even local distortions. It operates based on a set of parameters that determine the specifics of the registration process. These parameters are provided through a parameter file, a text file that describes the transformation model, optimization routine, and other specifics relevant to the registration procedure.

For the parameter file selection we consulted the Model Zoo, an online repository that archives several parameter files from past successful experiments. The site's organized catalogue (https://elastix.lumc.nl/modelzoo/) allowed us to browse through a variety of configurations that had been specifically optimized for brain 3D MRI data, which matched the nature of our atlas construction task.

It was essential to select parameter files that were designed for intersubject or interpatient registrations, rather than intrapatient, to ensure that the transformations would be suitable for the variations between different patients' brain scans. We focused on finding files that provided both rigid (1) and non-rigid transformation (2) parameters, so we could test each approach: the rigid transformations to align the overall structure and the non-rigid to adapt

to individual anatomical differences.

$$\begin{aligned} f_x(x,y,z) &= x \cdot \cos\theta + y \cdot \sin\theta + z \cdot \sin\phi + t_x \\ f_y(x,y,z) &= -x \cdot \sin\theta + y \cdot \cos\theta + z \cdot \sin\phi + t_y \\ f_z(x,y,z) &= -z \cdot \cos\phi + t_z \end{aligned} \tag{1}$$

In this equation:

- $f_x(x,y,z)$, $f_y(x,y,z)$, and $f_z(x,y,z)$ represent the transformed coordinates in the x, y, and z axes, respectively.
- The variables x, y, and z are the original coordinates.
- θ and ϕ represent the rotation angles around the x and y axes, respectively.
- t_x, t_y, and t_z are translation values in the x, y, and z directions.

This equation describes a rigid transformation for 3D images, including rotations and translations in all three dimensions.

$$\begin{aligned} f_x(x,y,z) &= a_x \cdot x + a_y \cdot y + a_z \cdot z + t_x \\ f_y(x,y,z) &= a_y \cdot x + a_y \cdot y + a_z \cdot z + t_y \\ f_z(x,y,z) &= a_z \cdot x + a_y \cdot y + a_z \cdot z + t_z \end{aligned} \tag{2}$$

The affine transformation equations represent the transformation of coordinates in three dimensions using coefficients a_x, a_y, a_z, and translation values t_x, t_y, t_z. The f_x, f_y, and f_z functions denote the transformed coordinates in the x, y, and z dimensions, respectively.

Although these parameter files are readily available for use, they are not one-size-fits-all solutions. Recognizing this, we downloaded several promising candidates and after conducting initial experiments, we manually adjusted these parameter files.

`Transformix`, on the other hand, is a tool that applies the transformations obtained by elastix to new data. Once an image has been successfully registered and the transformation parameters have been computed, transformix can be used to apply this transformation to other images or points of interest within the same coordinate system.

According to the `elastix` manual, and as we are using windows, downloading the precompiled files are the easiest way to start running the commands. So following instructions, we opened a CMD window in windows OS to run the basic command `elastix -f fixedImage.ext -m movingImage.ext -out outputDirectory -p parameterFile.txt` where fixedImage is the path to the image chosen as fixed, movingImage is the moving image, outputDirectory sets where the final result is stored and finally the parameter file. In our case, considering we were given each image mask, we tried using an additional parameter `-fmask` which is the path to the fixed image mask. According to the manual this can be helpful as it focus the registration to specific regions delineated within the brain volumes. This can be achieved setting the additional parameter `(ErodeMask "true")`.

The registration process initiated by deploying the command sequence that designated image '1012.nii' as the fixed reference and '1002.nii' as the moving image that required alignment. This operation was directed towards a specific output folder. The registration was structured as a multi-phase procedure, utilizing two distinct parameter files: 'Par0033rigid.txt' and 'Par0033similarity.txt'[1] [2] [3].

Output consisted in the iterations done by `elastix` as text files, a log file and an output file reflecting the changes done by the registration function. User can decide if an output

image is required or just the TransformParameter output file. TransformParameter file has the necessary info so `transformix` transforms another image with previous registration parameters. Output will have as much TransformParameter txt files as parameterFiles in the input of the `elastix` command.

Next step is called 'Label Propagation' in which groundtruth labels of moving images are transformed according to the TransformParameter of the registration process. This will help us to have not only the image transformed to the fixedImage space but also to standardize the labels.

2.3 Overall registration

After performing one example registration, we decided to automate the process by using a shell script on windows. However, the final process was done using Python (code provided). The result of the registration can be seen in the following image:

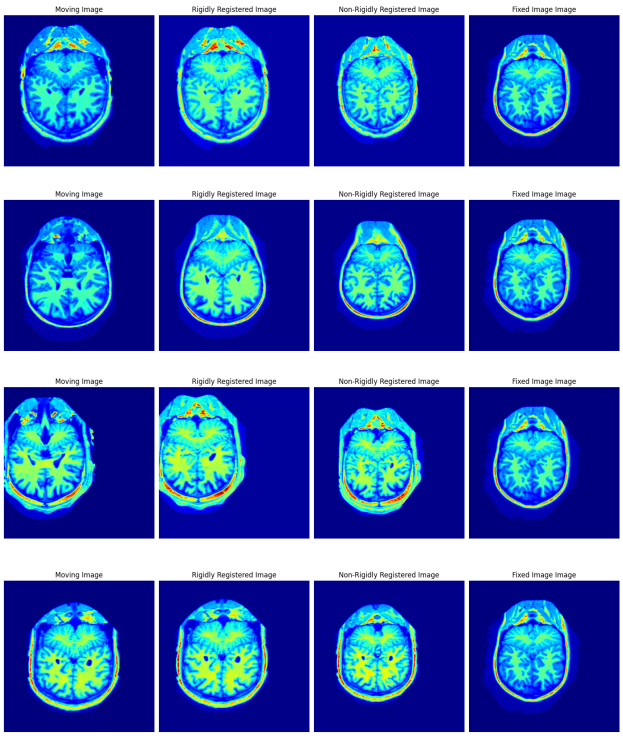

Figure 2: Result of rigid and non-rigid registration for images 1000, 1001, 1002 and 1006.

Once all the image were registrated, label propagation was done with the TransformParameters obtained. At first, we got an issue with the propagated label, which was giving labels with float type results data, which was not correct considering the labels are integer numbers 1, 2 and 3. After tutoring and further inspection of the TransformParameter file, we learned how to adjust the interpolator type and parameter values in order to have consistent values. Since we are working with label maps, it is crucial to use nearest neighbor interpolation to maintain the label values and this was achieved by setting `(FinalBSplineInterpolationOrder 0)`. Finally, since the final requested result was to deliver a NiFTI file, this parameter was also adjusted `(ResultImageFormat "nii")`. Otherwise, the default output value is `*.mhd`.

After having all registered images, we summed all image to have an average intensity voxel image as per the required objectives of the class. We did the same for each of the tissues, to have a probabilistic label probability per tissue.

3 Experimental section and results analysis

Following the steps described in the previous section, we proceeded to build the probabilistic atlas. First, we had the mean intensities overall image which is nothing more than a NiFTI file that has the average intensity of the sum of all resultant images after the registration and can be seen in the following figure:

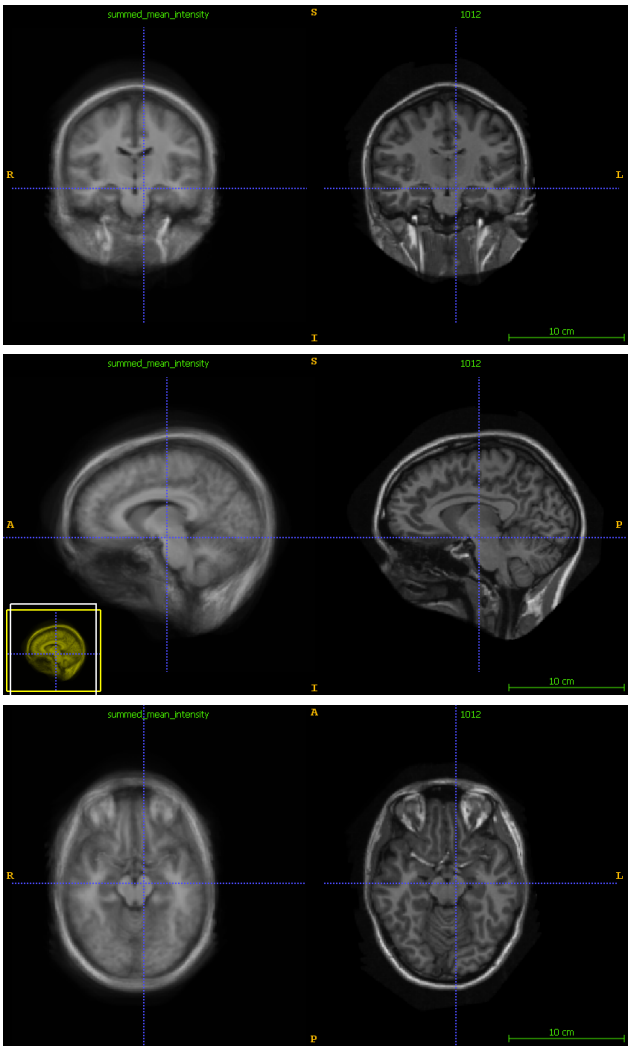

Figure 3: mean intensities in different planes compared to fixed image

As part of the experiments, and even if this is not the desired atlas, we also did the same average but with the propagated labels, to have an overview of the result of `transformix` and we obtained the following result:

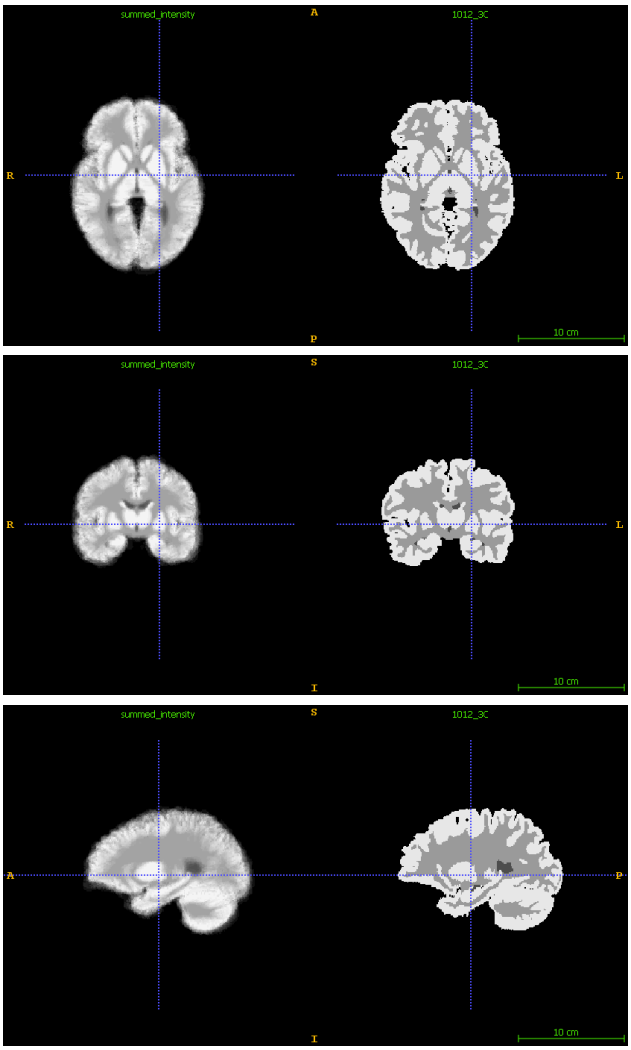

Figure 4: mean label intensities of the propagated labels in different planes compared to fixed image

In constructing the probabilistic atlas for brain tissue segmentation, we separated each tissue label by applying each transformed label mask to each corresponding registered moving image. This process involved overlaying the mask onto each image to isolate the specific tissue types—label 1 for cerebrospinal fluid (CSF), label 2 for white matter (WM), and label 3 for gray matter (GM). After the segmentation, we aggregated the data by summing the

masked regions across all images and then computed the average to construct a representative probability map for each tissue type.

For visualization, we generated plots that delineate the distribution of each tissue label. This serves as a check for the registration and labeling process. The resulting image, as displayed below, illustrates the averaged probability maps for CSF, white matter, and gray matter, each demarcated by distinct labels for ease of verification and interpretation. In the figure we used the fixed image label mask in background and the probabilities in color so the difference can be seen.

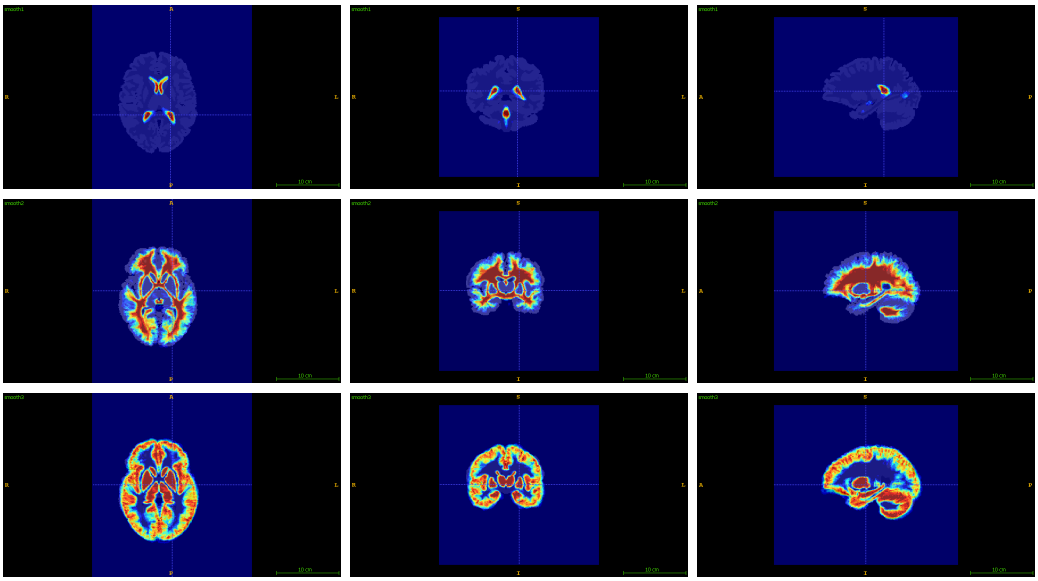

Figure 5: Label probabilities for each tissue. Top:CSF, middle: WM, bottom: GM

In our different experiments of constructing a comprehensive probabilistic atlas, we also tried an alternative approach by applying the fixed image mask directly to the mean intensities atlas. This strategy diverged from our initial method of aggregating each tissue type individually. The rationale behind this technique was to examine the mean intensities within the predefined regions of interest demarcated by the mask, which corresponds to the

different tissue labels.

The forthcoming image showcases the outcome of this method. While this approach yielded a visually ”cleaner” result, it inherently imposed a limitation by strictly confining the analysis to the mask's boundaries. Consequently, this might not truly reflect the nuanced variations and potential misalignments that naturally occur due to individual differences in brain anatomy and the inherent challenges of image registration, even if the target is having the most perfect and possible registration to a fixed image. Nonetheless, observing the mean intensities within the mask provided an intriguing perspective, offering a stark contrast to the probabilistic maps obtained by tissue-specific aggregation. Although this method may not capture the full complexity of brain morphology, it was a valuable exercise to visualize the extent of alignment within the regions of interest.

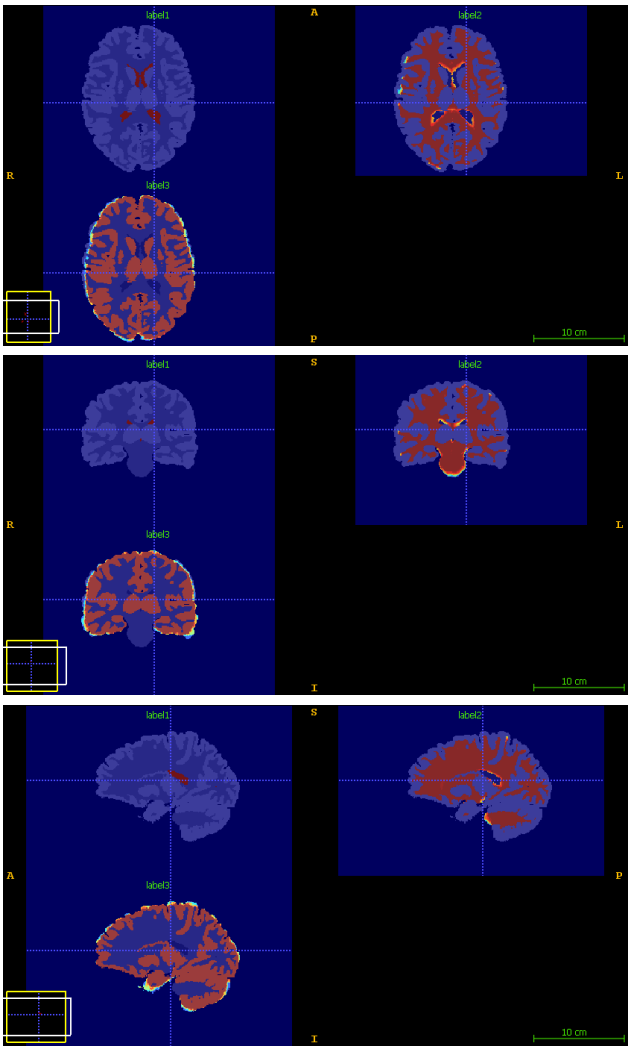

Figure 6: Label probabilities using mean intensity atlas and fixed image mask

3.1 Tissue Models

The subsequent phase in our analysis involved developing models of tissue intensity distributions of the original image. This was achieved by applying the fixed image labels as masks to the original image, allowing us to isolate and analyze the intensity values specific to each tissue type. By doing so, we gained insight into the unique distribution patterns that

characterize each tissue. Following this segmentation, we proceeded to normalize the intensity values to facilitate a more standardized comparison. The results of this normalization process are presented below:

Table 3: Statistical Summary of Tissue Intensity Data

Tissue Type	**Mean**	**Standard Deviation**
Non-Normalized Data		
CSF	651.76	237.07
White Matter	1507.35	161.26
Gray Matter	963.96	191.34
Normalized Data		
CSF	0.48	0.17
White Matter	0.66	0.07
Gray Matter	0.49	0.10

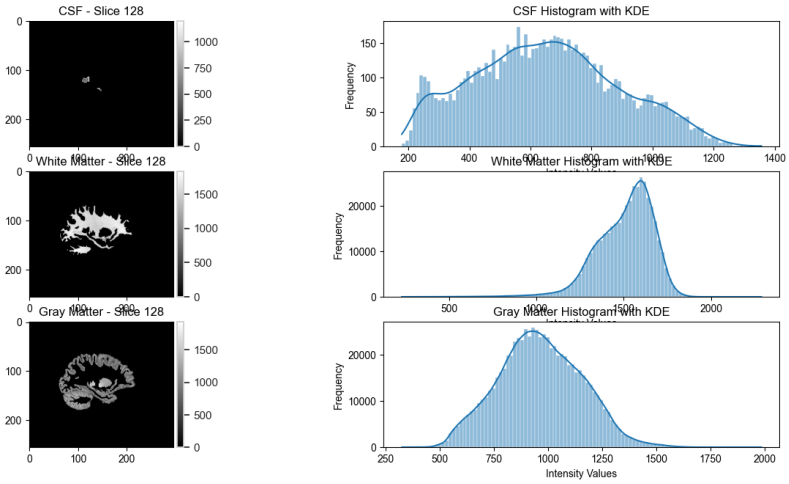

Figure 7: Tissue models

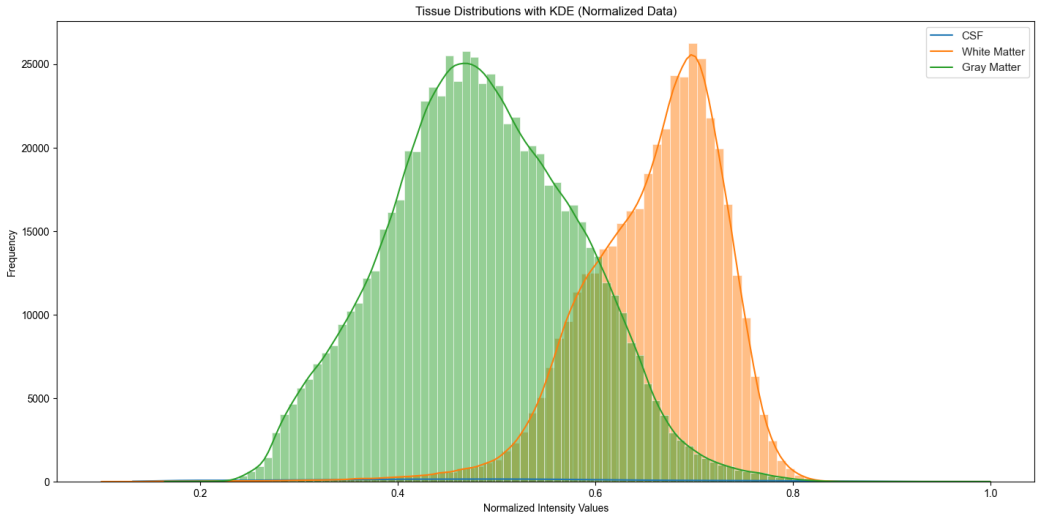

Figure 8: Normalized intensity tissue models

Then we computed the histogram distributions for each tissue type within the atlas of mean intensities. This step was helpful in providing a visual representation that allowed us to compare the distribution profiles of the tissues in the atlas against those in the original image. By examining these histograms, we could assess the consistency and variation between the derived atlas and the source data, offering valuable insights into the accuracy and quality of our atlas construction process.

Table 4: Tissue Intensity Distributions in the Atlas

Tissue Type	**Mean**	**Standard Deviation**
Non-Normalized Data		
CSF	567.26	235.05
White Matter	1204.80	205.44
Gray Matter	887.07	213.22
Normalized Data		
CSF	0.40	0.16
White Matter	0.77	0.13
Gray Matter	0.58	0.14

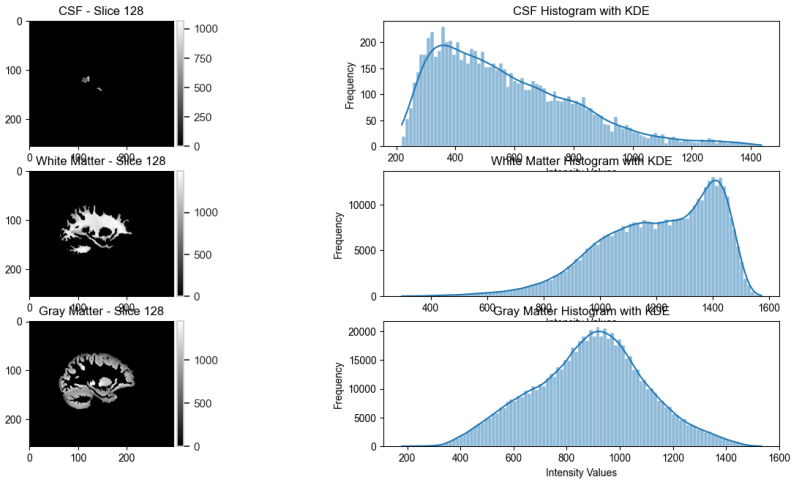

Figure 9: Tissue models in the mean intensity atlas

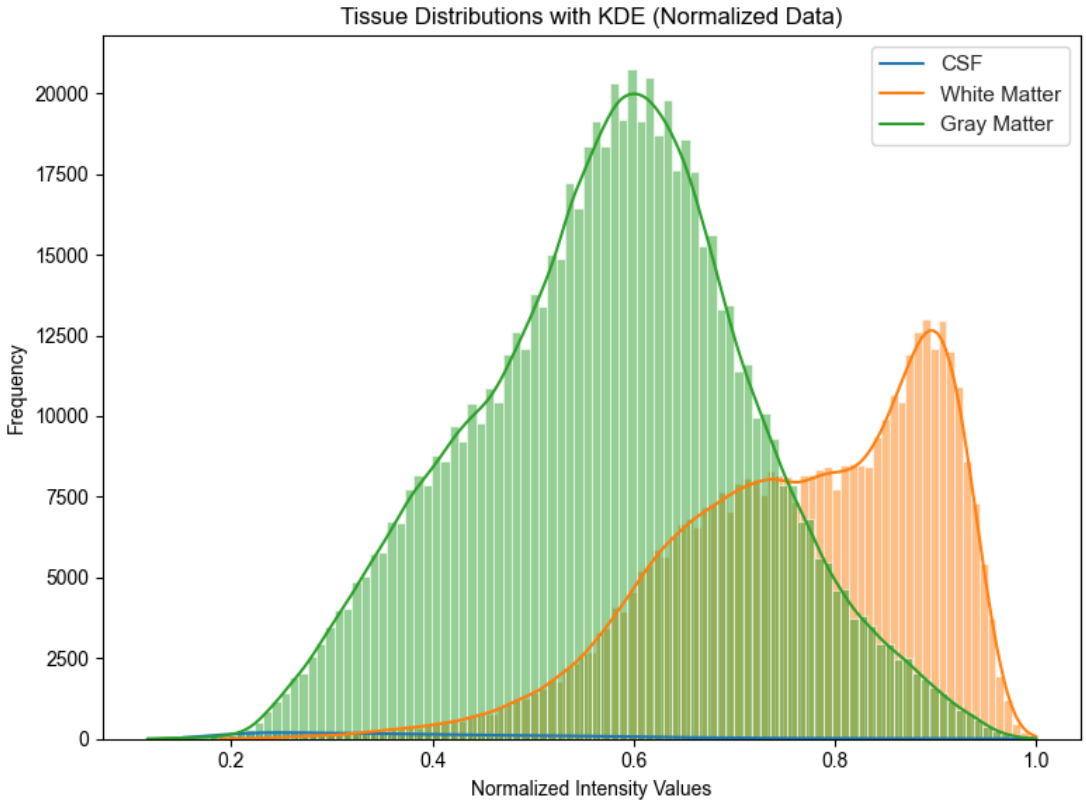

Figure 10: Normalized intensity tissue models in the mean intensity atlas

However, given the nature of CSF distribution, re-scaling the Y axis was necessary in order to appreciate all the tissues. This was done so the sum of all the y values are 1.

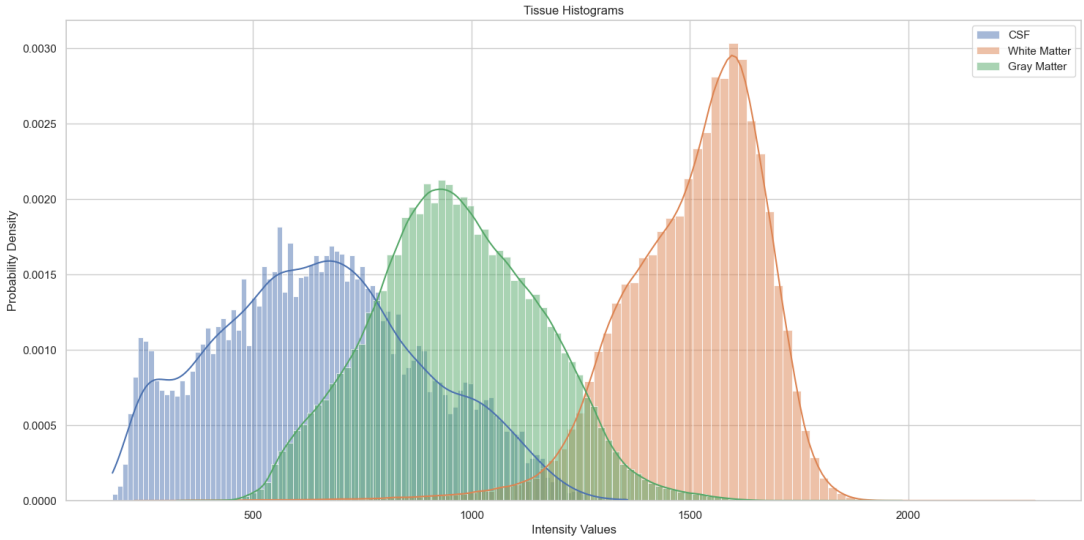

Figure 11: Tissue models in the fixed image

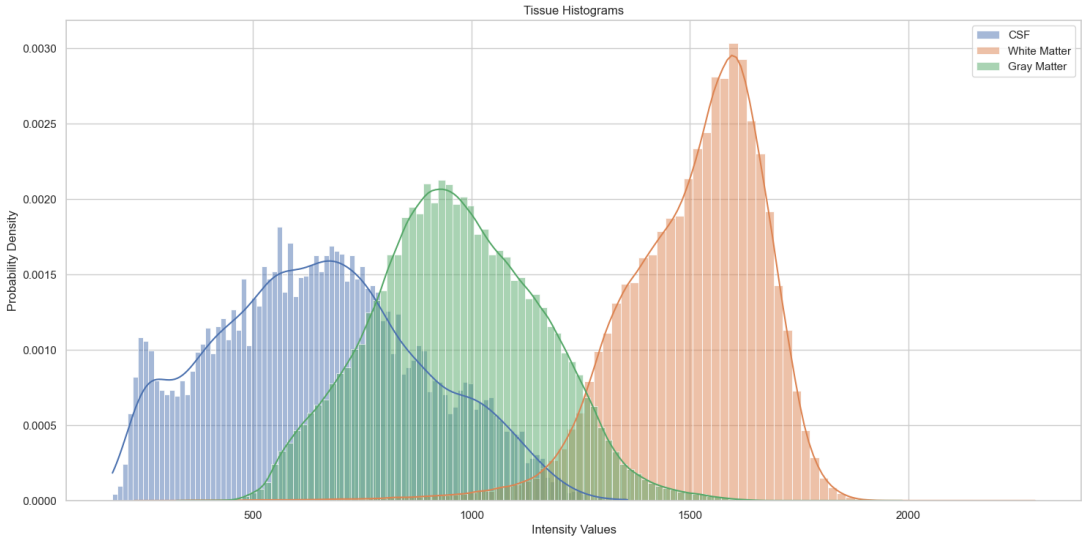

Figure 12: Tissue models in the atlas

4 Project management

In the project's initial phase, our primary focus was to gain a comprehensive understanding of the Elastix framework. This phase entailed dedicating approximately 4-5 days to reading the manual and conducting coregistration tests on the images. Following this, we optimized the workflow by automating the coregistration process for all images, aligning them with a randomly selected reference image. Additionally, we delved into various parameter configuration files from the Elastix Model Zoo.

Subsequently, we invested two days in implementing multiple approaches to identify the optimal reference image, ultimately selecting image 1012 based on the Dice score. The next phase was centered on developing and debugging the code specifically for building the atlas from the coregistered images, involving summation and averaging. During this phase, we also focused on software engineering principles to ensure clean and efficient code.

Finally, we ventured into creating histogram tissue models, which proved to be a challenging endeavor. This phase extended until deadline, due to difficulties related to the normalization concept.

5 Conclusions

The results obtained from this implementation yield valuable insights. It is clear that by leveraging available data alone, we can create probabilistic brain MRI maps without the reliance on external sources. This is accomplished through a twofold process, involving coregistration of images and the amalgamation of pixel distributions, followed by a crucial normalization step. What's particularly noteworthy is that, even with a limited number of acquisitions—illustrated here by our use of just 15 images—it is entirely feasible to construct

a highly useful atlas directly from these images. This atlas serves as a valuable resource for conducting in-depth analyses and deriving insightful inferences, particularly within the realm of clinical studies where the its focus centers on their intrastudy variations. Additionally, it proves invaluable in the creation of specific templates, enabling the generation of pathology- or pathophysiology-specific probabilistic maps using damaged brain images or functional modalities, greatly enhancing our understanding of these conditions. Incorporating ground truth information regarding the structures within the images, the segmentation procedure can be extended by formulating tissue probabilistic maps and modeling the distribution of these tissues. This approach enhances the accuracy and generalizability of the segmentation process, allowing for more precise and reliable results.

References

[1] Viktor van der Valk. *Par0033 - elastix*. URL: `https://elastix.lumc.nl/modelzoo/par0033/`.

[2] D.I. Bink et al. "Neuropathology in mouse models for atherosclerosis". Submitted 2016.

[3] B. Kogelman et al. In preparation 2016.